National gridded drought factors and comparison of two soil moisture deficit formulations used in prediction of Forest Fire Danger Index in Australia

Klara Finkele and Graham A. Mills
Bureau of Meteorology Research Centre, Australia, and Bushfire Cooperative Research Centre, Australia

and

Grant Beard and David A. Jones
National Climate Centre, Bureau of Meteorology, Australia

(Manuscript received December 2005; revised May 2006)

The operational calculation of Forest Fire Danger Index (FFDI) in the Australian Bureau of Meteorology requires the calculation of a 'Drought Factor' to represent fuel dryness. These calculations have hitherto only been calculated at a network of observing sites, where the data to both calculate and to verify forecasts of the FFDI are available. With the advent of increasingly more accurate and higher resolution numerical weather prediction models, forecasting the spatial distribution of the FFDI is desirable. Therefore, in order to duplicate operational forecast practice, but in a spatially distributed way, the spatial distribution of soil moisture deficit over Australia, using either the Keetch-Byram Drought Index (KBDI) or Mount's Soil Dryness Index (SDI) formulations, has been calculated at daily intervals on 0.25° (25 km) grids over Australia, and 0.1° (10 km) grids over southeastern Australia. In addition, the 'Drought Factors' based on the two soil moisture deficits and recent rainfalls are also computed on the same grids. The comparison of the two soil moisture deficit schemes shows that the main difference between the two is due to the treatment of evapotranspiration. SDI generally leads to higher soil moisture deficits, which in turn leads to a higher drought factor. This is especially the case at warmer inland locations, where the SDI is significantly higher than the KBDI due to the increased evapotranspiration. The analyses described in this paper make it possible to provide a range of fire weather related products to forecasters and clients on a national scale. Examples of such products are presented in this paper. In addition, using the National Climate Centre national daily rainfall and maximum temperature analyses since 1965, a 40-year archive of national soil moisture deficit and drought factor analyses has been generated and examples of the way this climatology can be used in operations are presented.

Introduction

Both short-term and longer term antecedent weather conditions affect fire behaviour in terms of their direct effects on a fire, and also through their effects on the moisture content of the fuels. In the Australian Bureau of Meteorology (the Bureau) the McArthur Forest Fire Danger Index (FFDI, Luke and McArthur 1978) is calculated operationally. It includes the very short-term response (drying) of fine-fuel moisture content due to

Corresponding author address: Graham A. Mills, Bureau of Meteorology Research Centre, GPO Box 1289, Melbourne, Vic. 3001, Australia.
Email: g.mills@bom.gov.au

changes in subdiurnal weather conditions (via the temperature and relative humidity terms), and also the longer-term response to antecedent conditions of the fuels in the deep litter bed via the so-called 'Drought Factor' (DF; Sullivan 2001). (While drought may have many different meanings in agricultural or hydrologic applications, DF will only have the McArthur FFDI meaning in this paper.) This DF is derived from either the Keetch-Byram Drought Index (KBDI, Keetch and Byram 1968) or Mount's Soil Dryness Index (SDI, Mount 1972) depending on agreed practice in each State. Operationally in the Bureau, the FFDI, and implicitly the DF, is calculated at a network of point locations at which the necessary observations for both calculation and forecast verification are available. Even though the determination of the FFDI is point-based, the determination of, for instance, a Fire Weather Warning (issued when FFDI > 50) is for regions and is area-based. The forecaster implicitly, or explicitly with the aid of spatially interpolated point forecasts of FFDI (e.g. in Tasmania and Western Australia), develops an area assessment based on the point data.

While the current operational fire weather forecasts are station-based, an increasing amount of forecast guidance is being presented spatially via mesoscale NWP model fields, and at resolutions much higher than the spacing of the observation network. By applying the operational station-based DF algorithms to the Bureau spatial (gridded) analyses of daily rainfall and maximum temperature (Weymouth et al. 1999; Jones 1999), national DF fields can be generated on regular arrays. These products provide forecasters and land managers with gridded daily analyses of SDI, KBDI and DF. In addition, gridded forecasts of the FFDI from the Bureau's mesoscale NWP models can be calculated using the appropriate spatial DF fields as input. It might be argued that the KBDI and SDI formulations of soil moisture deficit (SMD) are less sophisticated than the complex land-surface models being currently used in and developed for operational NWP systems, but in this paper we limit the analysis to the implementation of these operational formulations in order that the spatial products developed be directly comparable to the station values currently forecast.

The first purpose of this paper is to describe the development of such daily products, and also to provide a climatology of these daily fields based on the daily rainfall and maximum temperature analysis climatologies generated in the Bureau's National Climate Centre (NCC). Second, a nationally based comparison between the two SMD calculations and their resulting drought factors is presented, and the underlying reasons and consequences of the differences between the two formulations are discussed.

In the next section of this paper we present the process used to calculate the DF in current Bureau operations, using either KBDI or SDI, as this forms the basis for the gridded calculations. Further sections describe the additional features required in order to apply these algorithms to generate gridded DF fields, and present examples of the calculated fields, then analyse the factors that lead to different (generally higher) DF values when the SDI is used instead of the KBDI, and finally present examples of applications of the output to fire weather forecasting.

Soil moisture deficit and drought factor calculations

The drought factor is an estimate of the dry fuel moisture content or, equivalently, the amount of dry fuel available for burning. It is calculated by combining estimates of the effects of (a) direct wetting from recent 'significant' rainfall; and (b) wetting from below, which is dependent on the soil moisture content. The contribution of the second effect is calculated as a soil moisture deficit, using either the Keetch-Byram Drought Index (KBDI) (Keetch and Byram 1968) or the Soil Dryness Index (SDI) (Mount 1972). The soil moisture balance and drought factor are determined on a daily time step. Only the relevant details for the comparison of the two schemes will be presented in this paper and for further details of the calculations see Finkele et al. (2006).

Soil moisture deficit (SMD)

In both the KBDI and the SDI, the water balance is expressed in terms of the SMD, which is the amount of water in millimetres necessary to bring the soil moisture content back to field capacity, i.e. the amount of water the soil can hold in its capillaries against gravity. A low SMD therefore means there is little or no constraint to evaporation from soil or transpiration from plants, and also little capacity for infiltration in the case of heavy rainfall. A high SMD means that there is very little water available for either soil evaporation or plant transpiration. Both the KBDI and the SDI models assume a maximum soil moisture deficit of 200 mm and a minimum soil moisture deficit of zero. While some water balance models will allow the soil moisture to exceed the field capacity (negative soil moisture deficit) neither KBDI nor SDI formulations allow this, and there is no allowance for deep drainage in either case.

In general terms, the soil water balance is determined by the difference between the amount of water infiltrating into the soil, called effective rainfall in this context, and the evapotranspiration, which is the

amount of water leaving the soil either via transpiration from vegetation or via evaporation from the soil. The changes in SMD are thus expressed as

$$\frac{d\,SMD}{dt} = -P_{eff} + ET \qquad ...1$$

where t is the time step (1 day), P_{eff} is effective rainfall (mm day^{-1}), which decreases the soil moisture deficit, and ET is evapotranspiration (mm day^{-1}), which increases the deficit. While each of the soil moisture models follows Eqn 1 in its general form, their detailed formulations of P_{eff} and ET differ and are presented in Table 1.

The KBDI is widely used in Australia, and is used operationally in the New South Wales, Victoria and Queensland Regional Offices of the Bureau for calculating DF. There are five underlying assumptions inherent in the formulation of KBDI (Sullivan 2001):

(a) The rate of moisture loss from the soil is a function of vegetation cover, which itself is a function of mean annual rainfall.
(b) The vegetation-rainfall function is approximated by an exponential curve and moisture loss is a function of mean annual rainfall.
(c) The rate of moisture loss from soil is determined by the evapotranspiration.
(d) The rate of moisture loss from soil is approximated by an exponential decay curve in which the wilting point is the lowest moisture level.
(e) The soil depth is such that it has a field capacity of 200 mm.

The daily effective rainfall is based on the previous 24-hour rainfall amount (rain in Table 1) decreased by an amount to allow for interception and runoff. The interception and/or runoff is approximated for KBDI as the first 5 mm within consecutive days with non-zero rainfall. This is irrespective of ground cover and no distinction is made as to whether this is due to interception on vegetation cover and/or surface runoff.

The evapotranspiration ET depends on the previous day's soil moisture deficit $KBDI_{n-1}$, the previous day's maximum temperature $T_{\max}$, and the annual rainfall R_{annual}. A typographical error occurred in the original Keetch and Byram (1968) publication and has been noted by several authors (Sullivan 2001). The corrected formula is shown in Table 1.

The second soil water balance model used in Australia is the SDI, which was developed in Tasmania by Mount (1972) as a rainfall-runoff model and was based on the KBDI. The operational drought factor calculations in South Australia and Tasmania are based on the SDI, while SDI is used to estimate prescribed burning conditions in Western Australia. Infiltration and runoff are calculated separately in the estimation of daily effective rainfall (Table 1), and are vegetation cover dependent. The SDI requires a Vegetation Class to be defined at each calculation point, and for each Vegetation Class a canopy rainfall interception fraction (R), a canopy storage capacity (C), a canopy loss per wet day (W), and a Flash Runoff fraction (FR) are defined (Table 2). The vegetation class O represents lakes, rock and bare soil. The vegetation classes A-F depend on the vegetation type (eucalypt or pine), understorey density and tree canopy. Observing stations in South Australia, Tasmania, Victoria and Western Australia have been assigned a subjectively assessed vegetation class according to the Mount (1972) guidelines. The extension from station classification to grid-point classification is discussed in the section on static input data.

The amount of rainfall intercepted by the canopy is dependent on the previous day's canopy water store, canopy storage capacity C, canopy rainfall interception fraction R and the canopy loss per wet day W. The canopy water balance is determined by the interception and loss by evaporation from the wet canopy on consecutive wet days. The canopy store is assumed to dry completely in a single dry day following a series of wet days. The runoff is a fraction of rainfall according to the vegetation class.

Table 1. Water balance components determining the soil moisture deficit for KBDI and SDI on day n: effective rainfall (P_{eff} in mm day^{-1}), evapotranspiration (ET in mm day^{-1}), rain (24-hour rainfall amount). $KBDI_{n-1}$ and $T_{\max}$ are the previous day's soil moisture deficit and maximum temperature respectively, R_{annual} is the mean annual rainfall, and a_i and b_i are derived coefficients. For KBDI the run-off and interception processes are not treated separately as is the case of SDI.

	KBDI	*SDI*
P_{eff}=	rain – (interception, run-off)	rain – interception – run-off
ET=	$\dfrac{(203.2 - KBDI_{n-1})(0.968e^{(0.0875T_{\max} + 1.5552)} - 8.3)}{1 + 10.88\,e^{-0.00173R_{\text{annual}}}}10^{-3}$	$a_i\,T_{max} + b_i$

Table 2. Vegetation class characteristics after Mount (1972).

Vegetation class	*O*	*A*	*B*	*C*	*D*	*E*	*F*
Integer value	*1*	*2*	*3*	*4*	*5*	*6*	*7*
Canopy rainfall interception fraction *R*	0	0.1	0.2	0.3	0.4	0.5	0.6
Canopy storage capacity *C*	0	0.5	1.0	2.0	2.5	3.5	4.0
Canopy loss per wet day *W*	0	0.5	0.5	0.5	0.5	0.5	1.0
Flash run-off fraction *FR*	1/10	1/20	1/30	1/40	1/50	1/60	1/70

The evapotranspiration for SDI is estimated by a linear function of maximum daily temperature T_{max} (Table 1), where the coefficients a_i and b_i have been derived from the relationship between average monthly maximum daily temperature and monthly tank evaporation in capital cities. The coefficients vary with temperature and soil moisture deficit range and these relationships are explored in Finkele et al. (2006). For the Bureau's operational implementation of the SDI, these coefficients were only derived for the southern states; therefore the SDI maps will only be shown for the southern half of Australia.

Drought factor

The drought factor (*DF*) is calculated using the 'improved' formula developed by Griffiths (1998) and is based on the soil moisture deficit (either KBDI or SDI) and the past 20 days' rainfall. It is obtained as

$$DF = 10.5(1 - e^{-(SMD + 30)/40}) \frac{41x^2 + x}{40x^2 + x + 1} \qquad ...2$$

where the variable x expresses the influence on the drought factor of the past rainfall amount (P) and number of days since it fell (N). It is calculated as

$$x = \begin{cases} \dfrac{N^{1.3}}{N^{1.3} + P - 2} & N \le 1 \text{ and } P > 2 \\ \dfrac{0.8^{1.3}}{0.8^{1.3} + P - 2} & N = 0 \text{ and } P > 2 \\ 1 & P < 2 \end{cases} \qquad ...3$$

To determine the significant rainfall event during the past 20 days, the function x is minimised over P and N. A rainfall event is defined as a set of consecutive days, each with rainfall above 2 mm. The rainfall event amount P is the sum of rainfall within the event. The event age N is defined as the number of days since the day with the largest daily rainfall amount within the rain event. This definition of event age has been used by Forestry Tasmania when implementing the FFDI Mark 5, and it has been adopted by most States using the SDI (Sullivan 2001). Another interpretation of event age is to assume the accumulated rainfall amount fell on the last day of the event. However, this leads to an underestimation of the drought factor as any drying during the rain event is ignored with this assumption.

In operational use it was found that the above algorithm tended to increase the drought factor too quickly in prolonged dry periods following a significant rain event. This tendency has been ameliorated in the Bureau's operational calculations, by substituting x with the minimum of the two quantities, namely the previously calculated x as in Eqn 3 and the limiting function x_{lim}, where

$$x_{lim} = \begin{cases} \dfrac{1}{1 + 0.1135\ SMD} & SMD < 20 \\ \dfrac{75}{270.525 - 1.267\ SMD} & SMD \ge 20 \end{cases} \qquad ...4$$

This substituted value of x is then used to calculate the drought factor in Eqn 2. Note the coefficient in the drought factor calculation in its original algorithm (Eqn 2) is 10.5, which can result in a drought factor beyond the maximum value of 10, and the adjusted drought factor using the functional form x_{lim} can also be larger than 10. Using either formulation, the final DF needs to be limited to be less than the maximum drought factor of 10 (i.e. DF=min(10, $DF_{Eqn\ 2}$).

Gridded soil moisture deficit and drought factor

In this section we describe the manner in which gridded fields of SMD and DF have been generated, providing a regularly distributed field of DF covering the whole of Australia rather than the irregular point-based data hitherto available. In doing this, we have chosen to calculate the DF from regular arrays of the input ingredients, but using the algorithms described in the preceding section. These inputs fall into two broad classes:

(a) Daily input data: daily rainfall and maximum temperature analyses.
(b) Static input data: annual rainfall and vegetation classification fields.

These input data sources, and examples of the output fields are described and presented in this section.

Daily input data

The daily input data necessary for both the KBDI and the SDI are daily rainfall and daily maximum temperature analyses. The Barnes successive correction method analysis of daily rainfall (Weymouth et al. 1999) is available for all of Australia on a 0.25° (approximately 25 km) grid, and over the southeastern part of Australia, where the observation network is sufficiently high to support a more detailed analysis, on a 0.1° (approximately 10 km) grid. The daily rainfall analysis is produced in real time with some 1200 reports potentially available nationally, and with some 600 potential reports for the southeastern Australia analysis. In non-real time, some 5000 to 6000 reports are received, and the NCC produces a 'final' rainfall analysis utilising this larger amount of data some six months after the event. In some parts of the country, mainly the desert regions of Western Australia (Gibson Desert and Great Victorian Desert) and the Northern Territory (Simpson Desert), the sparsity of the rainfall observation network makes an objective analysis (interpolation of data to a regular grid) problematic, and these areas are flagged in the analyses. As the calculation of DF is intended to apply to the calculation of Forest FDI, the unavailability of the KBDI/SDI in these regions does not limit the aims of this project.

A gridded daily maximum temperature analysis, using approximately 700 stations, and covering all of Australia, is produced in real time on the same 0.25° (approximately 25 km) grid by the NCC, again using the Barnes successive correction technique (Jones 1999). This 0.25° grid is interpolated to the 0.1° southeastern Australia rainfall grid to provide a compatible maximum temperature analysis for this area.

It has to be kept in mind when interpreting the SMD and DF maps, that they are based on input data which is spatially representative at either the 0.25° or 0.1° scale, and will not necessarily exactly match the individual observations used in the analysis. This issue is described in detail by Weymouth et al. (1999). Under some circumstances the difference in the rainfall amount between the value representing a 0.25° grid cell and the point location can be large, such as in complex terrain or in convective small-scale rain events. The difference in maximum temperature between grid value and point value is generally rather smaller due to the greater spatial homogeneity (and perhaps also to the less-dense observation network) of the maximum temperature observations. Finkele et al. (2006) present examples of the scatter between the observations of rainfall and maximum temperature at Cranbourne, Victoria, and the respective analysed values at that location for August 2003 to August 2004. There is little bias or scatter in the temperature data. However, there is considerably greater scatter between the analysed and observed rainfall observations, together with a clear underestimation in the analysed rainfall values when the observed rainfall is greater than just a few millimetres. In this example the total rainfall for the 12 months is 780 mm for the grid value and 837 mm for the observation site. This difference in input data will result in different SMD and subsequently different drought factors.

Static input data

As well as the daily rainfall and maximum temperature fields, computation of the drought factor needs fields of mean annual rainfall for the KBDI, and of vegetation class for the SDI. In addition for the SDI the coefficients a_i and b_i are needed at each grid-point in order to calculate ET as a function of $T_{\max}$. The gridded mean annual rainfall is based on the Barnes analysis of monthly data from 1971 to 2000 and was supplied by the NCC.

The SDI vegetation class has been subjectively specified only for those observation stations at which SDI is calculated in Western Australia, South Australia, Victoria and Tasmania. Investigating various approaches to obtain a vegetation class at each grid-point, we have chosen to link Mount's vegetation cover (or interception) class to leaf area index (*lai*) data, since most current land surface parametrisation models describe interception as a fraction of *lai*. For the purpose of determining the vegetation classification as a function of *lai*, the 5 km vegetation dataset developed by Dean Graetz of CSIRO (personal communication) was available, as it is used by the Bureau's operational limited area numerical weather prediction model (LAPS, Puri et al. 1998) in its higher resolution configurations (e.g. Cope et al. 2004). This high resolution vegetation dataset was specifically developed for Australia in the early 1990s and has been validated by spot ground observations. To map Graetz's 31 vegetation classes to the seven vegetation classes of Mount, a numerical value of 1-7 was assigned to each Mount class O-F (Table 2). For all stations for which a Mount vegetation classification had been defined, the corresponding Graetz class was determined from the 5 km dataset. Not all Graetz classes are sampled by the operational stations for which Mount vegetation classes have been specified. For those Graetz classes for which corresponding

Mount classes were found, the average Mount class within each Greatz class is shown in Table 3. It was found that, for the Graetz classes for which matches with subjective (Mount) classes were available (Table 3), the linear relation

$$VegClass_{SDI} = \text{nearest integer } (lai + 1) \quad ...5$$

between Mount class and Graetz *lai* fit the data satisfactorily.

The SDI class of bare ground (O, numerical value 1) is assumed for $lai < 0.5$ and the SDI class representing light understorey and no tree canopy (A, numerical value 2) for *lai* between 0.5 and 1.5 etc. SDI is not calculated for oceans and lakes (Graetz class 0, 29 and 30) and therefore no SDI vegetation cover has been assigned. An exception was made for the urban class of Graetz dataset (31) where the average SDI class has been assigned rather than using the *lai* value and Eqn 5.

Given that there are some 25 'footprints' from the Graetz vegetation classes within one 0.25˚ grid-cell of the SDI grid, there is not necessarily a unique way to define which Graetz class should be used for an individual SDI cell. One could use the *lai* of the dominant vegetation type, use the maximum *lai* of any vegetation type within the grid cell, or simply average the *lai* within the grid cell. Using the maximum *lai* appears to overestimate the forested regions, in particular around the east coast and in Tasmania, while a vegetation type mapping based on the average *lai* leads to smoothing of the vegetation heterogeneity (e.g. Fig. 1). We have chosen to use the *la*i of the dominant vegetation type since that appears to provide a reasonable representation of the ground cover. It might be argued that as the DF is used for the FFDI calculation, it should be based on the forested part of the grid cell; however, it can equally be argued that the infiltration reducing the grid cell SMD will be better represented

Table 3. Mapping of Graetz vegetation classification to SDI interception classes using nearest integer of (*lai* + 1) and averages within a Graetz vegetation class of the existing SDI station data classifications.

Index	*Graetz Vegetation Class description*	lai	*nint(lai+1)*	*Average $VegClass_{SDI}$ within Graetz class*	*$VegClass_{SDI}$ estimate*
0	ocean	0	1		
1	tall dense forest	4.80	6	6.33	6
2	tall mid-dense forest	6.30	7	4.72	7
3	dense forest	5.00	6		6
4	mid-dense forest	3.75	5	4.33	5
5	sparse forest (woodland)	2.78	4	3.00	4
6	very sparse forest (woodland)	2.50	4		4
7	low dense forest	3.90	5		5
8	low mid-dense forest	2.77	4		4
9	low sparse forest (woodland)	2.04	3	3.67	3
10	tall mid-dense shrubland (scrub)	2.60	4		4
11	tall sparse shrubland	1.69	3	2.67	3
12	tall very sparse shrubland	1.90	3		3
13	low mid-dense shrubland	1.37	2		2
14	low sparse shrubland	1.50	3	4.50	3
15	low very sparse shrubland	1.21	2		2
16	sparse hummock grassland	1.58	3		3
17	very sparse hummock grassland	1.41	2		2
18	dense tussock grassland	2.30	3		3
19	mid-dense tussock grassland	1.20	2	3.65	2
20	sparse tussock grassland	1.71	3		3
21	very sparse tussock grassland	1.21	2	3.00	2
22	dense pasture/herbfield perennial	2.30	3	4.45	3
23	dense pasture/herbfield seasonal	2.30	3	2.22	3
24	mid-dense pasture/herbfield perennial	1.20	2	3.89	2
25	mid-dense pasture/herbfield	1.20	2	2.79	2
26	sparse herbfield	1.87	3	4.35	3
27	very sparse herbfield	1.00	2	3.00	2
28	littoral	3.00	4	2.50	4
29	permanent lake	0	1		0
30	ephemeral lake	0	1		0
31	urban	0	1	3.14	3

Fig. 1 **Three methods of assigning grid cell SDI interception classes to the 0.25° (approximately 25 km) grid (left column) and 0.1° (approximately 10 km) grid (right column). First method is assigning the dominant vegetation type *lai* as the grid cell class ((a) and (d)), the second method is assigning the maximum *lai* ((b) and (e)) and third method is assigning the average *lai* ((c) and (f)).**

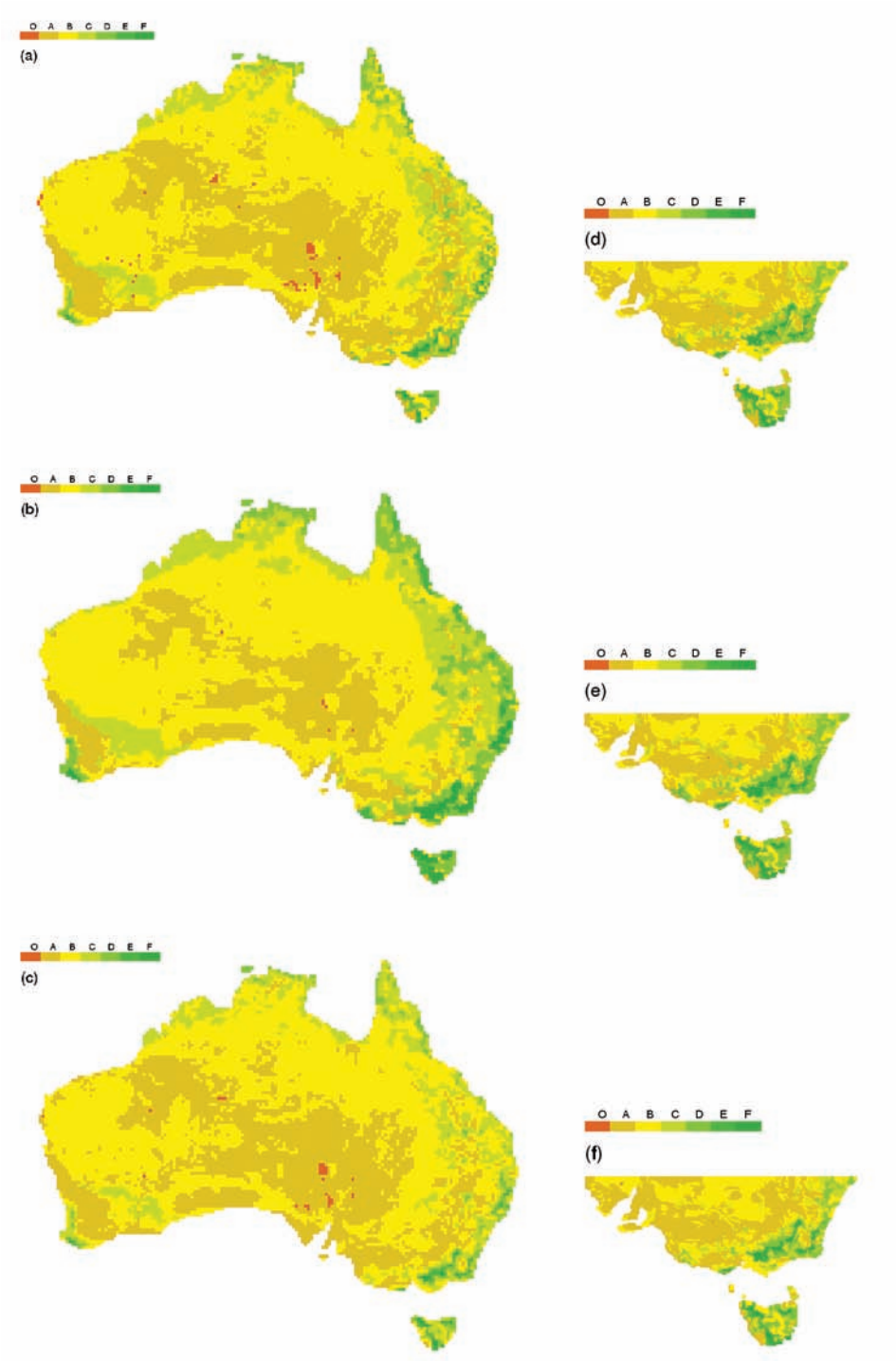

by the dominant vegetation type. This issue of assigning a vegetation type to a grid cell is scale-dependent, and clearly becomes less problematic as the size of the grid cells is reduced. This is evident when the 0.25˚ and 0.1˚ maps of SDI vegetation class using the three assumptions above are compared (Fig. 1).

The operational estimation of evapotranspiration for the SDI at observing stations has been based on regression coefficients a_i and b_i (Table 1) at State capital cities in South Australia, Victoria and Tasmania. In Western Australia the coefficients from South Australia are used. Given that these choices appear to be somewhat arbitrary, the calculation of the gridded SDI only uses one set of coefficients for the southern half of Australia for simplicity and to avoid discontinuities at State boundaries. At low SDI values the observations of evapotranspiration for Hobart and Melbourne are very similar and values for Adelaide are slightly higher. For high SDI values the observations are very close for all three capital cities. Assigning the coefficients from Adelaide would have overestimated the evapotranspiration at low SDI values, while using the coefficients from Melbourne would have overestimated the evapotranspiration at higher values of SDI; therefore, the coefficients from Hobart were chosen to calculate the evapotranspiration for SDI, but as this approximation clearly has its limitations, particularly in warmer climates, and as there are no current operational requirements for SDI in the northern part of Australia, we restrict these calculations to the southern half of Australia.

Daily and normal grids

Daily grids of the KBDI and DF based on the KBDI (DFK) are being produced for all Australia and the SDI and DF based on the SDI (DFS) for the southern half of Australia on the 0.25˚ grid, and for the southeast on the 0.1˚ grid. These fields are available shortly after completion of the daily temperature and rainfall analyses in the early afternoon. In addition the NCC has a set of daily rainfall and daily maximum temperature analyses available from 1965 onwards, and daily gridded KBDI, SDI and DF analyses based on the KBDI and the SDI have been produced for each day using these data. The operational daily production of the grids uses the real time rainfall analysis whereas the historical SMD and drought factor grids used the rainfall re-analyses from NCC (which use a much greater number of rainfall observations).

The daily SMD and DF grids from 1971 to 2000 have been used to produce annual mean and daily normal grids for both the 0.25˚ and 0.1˚ resolution grids. The daily normal grids have been filtered over 31 days to smooth out small-scale variations due to individual rainfall events. The daily normal grids also provide a reference for the current daily grids as the difference between the two gives an indication if conditions become exceptional for a particular time and location.

Comparison of KBDI and SDI and their respective DF

The upper pair of charts in Fig. 2 shows the annual average KBDI, SDI and their respective drought factor analyses for the 0.25˚ analyses, while the respective fields from the 0.1˚ analyses are shown in Fig. 3. It is clear that the SDI formulation leads to a higher mean SMD, and thus DF, over most of southern Australia than does the KBDI formulation. Given that the basic formulae are identical (Eqn 1), the differences result from the different methods used to calculate P_{eff} and ET (Table 1). We now examine the relative effects of the different approaches to the calculation of these two quantities.

The annual average daily evapotranspiration for the two schemes is shown in the third row of Fig. 2 for the 0.25˚ grid and of Fig. 3 for the 0.1˚ grid. In both cases the evapotranspiration for KBDI is highest in the high rainfall regimes along the eastern parts of Australia, the western parts of Tasmania and southeast Victoria. This can also be seen in Fig. 2 along the northern coastal parts of Australia. However, the evapotranspiration pattern for the SDI follows the spatial distribution of temperature and therefore is higher for the warmer inland parts of the country. The sum of the daily differences (actual and absolute) of the evapotranspiration (ET) and effective rainfall (P_{eff}) estimated by the two schemes for a selection of stations is shown in Table 4. (The locations of the stations are shown in Fig. 4.) The sums of the differences and of the absolute differences are the same except for Nambour, showing that the evapotranspiration for SDI is significantly higher than for KBDI at nearly all locations. Only at a few coastal locations on the mid to northeast coast is there a higher annual evapotranspiration for KBDI than for SDI.

The amount of rainfall actually infiltrating the soil after estimation of the amount lost due to vegetation interception and run-off is called the effective rainfall in this context of soil moisture deficit. The KBDI has a simple scheme whereby the first 5 mm of a rainfall event (consecutive days with non-zero daily rainfall) are lost due to either interception or surface run-off. No distinction is made between the two processes. SDI uses the vegetation class and its characteristics to determine the amount of rainfall being lost due to canopy interception and surface run-off.

Fig. 2 **Comparison between KBDI (left column) and SDI (right column) of 0.25° gridded annual average of drought factor, soil moisture deficit, annual daily evapotranspiration and effective rainfall.**

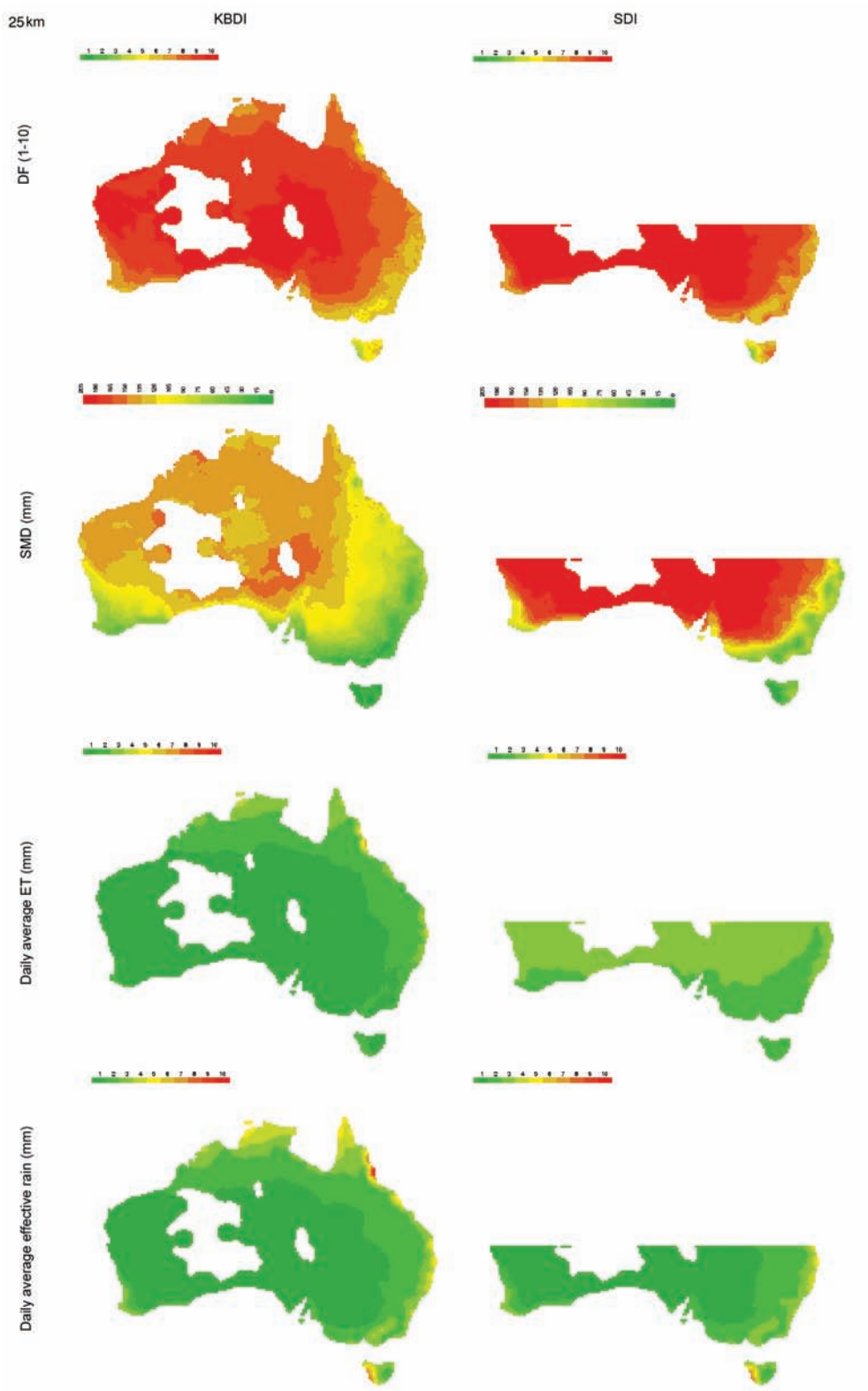

Fig. 3 **Comparison between KBDI (left column) and SDI (right column) of 0.1° gridded annual average of drought factor, soil moisture deficit, and annual daily evapotranspiration and effective rainfall.**

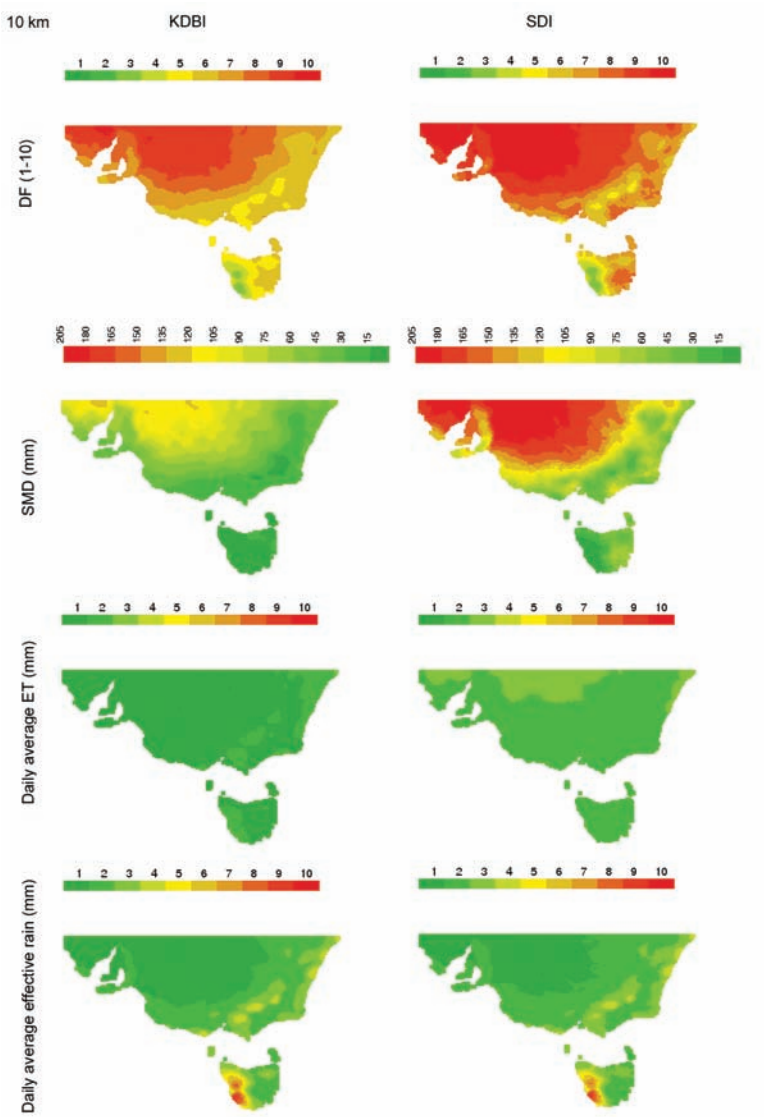

Depending on the size of the canopy storage, runoff coefficient and the frequency and size of rainfall events, the two schemes will result in slightly different effective rainfall amounts. For individual rainfall events of less than 5 mm the KBDI will estimate zero effective rainfall whereas SDI will estimate a non-zero effective rainfall. However, Figs 2 and 3 show that, on average, the difference between the two schemes is small. The sum of the daily differences and absolute differences of annual average effective rainfall of the two schemes can been seen at the station locations in Table 4. No clear pattern can be seen from the table, with some locations showing SDI having larger effective rainfall than KBDI (e.g. Clare, Mildura, Jacup) whereas other locations show the KBDI to have larger effective rainfall (e.g. St Helens, Dwellingup, Manjimup). Overall the effect of the difference in the effective rainfall is an order of magnitude smaller than that of the difference in evapotranspiration between KBDI and SDI.

The analysis presented immediately above shows that the SDI formulation will nearly always lead to higher soil moisture deficits than does the KBDI formulation (Figs 2, 3), due almost entirely to the much larger evapotranspiration term for SDI in the water balance equation (Table 4). Especially at warmer inland locations (e.g. Mildura), the SDI is significantly higher than the KBDI due to the greater calculated evapotranspiration there. This might point to the reason why SDI is generally believed to be only applicable in cool climate regions (J. Bally, personal communication) and seems to overestimate the soil moisture deficit in warmer inland regions with sparse vegetation. The SDI may not be appropriate at such locations, as the evapotranspiration does not take into account vegetation cover and is a linear function of maximum temperature with its coefficients derived at cooler mainly coastal locations.

As a result of the SDI being larger than the KBDI at almost all locations, the DF based on the SDI (DFS) is also larger than that based on the KBDI (DFK). However, averaging in time and over different drought factor classes can mask some of the difference between the KBDI and SDI. As an example, the mean annual cycle of DF as calculated from the two different SMD estimates is shown in Fig. 5 at three sample locations (Clare, Launceston and Bega). At Clare the average DF in summer shows little difference between the two schemes, although the gap is rather wider in the late winter/early spring. This pattern is reversed at Launceston, while DFK is uniformly less than DFS throughout the year at Bega.

Frequency distributions within drought factor classes also differ. Figure 6 shows the number of days per month for which the DF is less than 6, 7, 8, 9 and 10 for these three locations. Thus the length of a colour bar is an indicator of the relative frequency of DF in that range.

At Clare the difference is most pronounced at the higher end of the drought factor spectrum. At the lower end of the drought factor spectrum (0-6), which is important for prescribed burning conditions, both schemes yield similar results. However, the SDI shows significantly more days throughout the year, including in winter, with very high drought factors between 9 and 10. For the SDI there are very few days with intermediate drought factors and the distribution of drought factors is concentrated in either the low (0-6) or the high (9-10) end of the spectrum. However, for the KBDI the transition from low to high DF is somewhat more gradual and therefore virtually no days in winter with high drought factors.

Fig. 4 Map of the station locations listed in Table 4 for comparison of the two schemes.

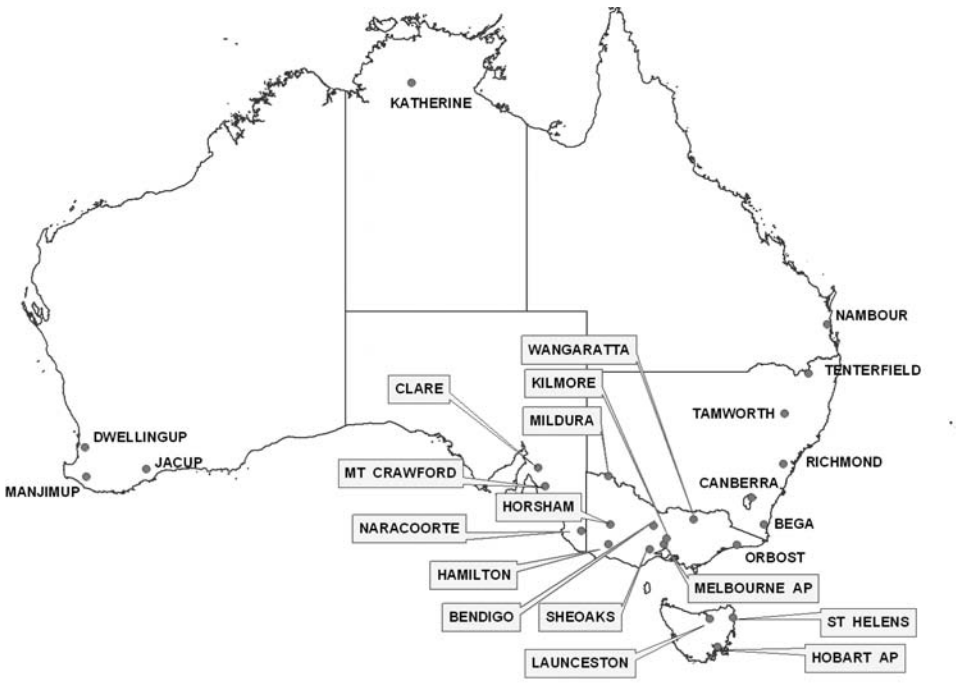

Table 4. Annual sum of the difference (actual and absolute) between daily average SDI and KBDI of evapotranspiration (ET in mm per year) and effective rainfall (P_{eff} in mm per year) for a selection of locations, extracted from the 0.25° gridded data.

Annual sum of daily *Station*	*ET SDI-KBDI*	*ET |SDI-KBDI|*	*Peff SDI-KBDI*	*Peff |SDI-KBDI|*
CLARE	363.9	363.9	49.8	49.8
MT CRAWFORD	290.9	290.9	15.8	38.6
NARACOORTE	306.2	306.2	8.9	52.3
MILDURA	509.0	509.0	72.2	72.2
HORSHAM AWS	328.4	328.4	55.7	55.7
HAMILTON AWS	286.3	286.3	4.5	47.0
BENDIGO	283.5	283.5	22.3	31.3
KILMORE GAP	285.3	285.3	-11.0	47.3
SHEOAKS AWS	317.2	317.2	13.8	40.6
WANGARATTA AWS	320.6	320.6	39.9	47.9
MELBOURNE AP	336.1	336.1	12.8	38.2
ORBOST AWS	276.5	276.5	75.6	75.6
HOBART AP	329.8	329.8	-23.7	38.2
LAUNCESTON	342.7	342.7	-14.2	40.7
ST HELENS AERO	317.3	317.3	-36.0	40.2
BEGA	264.5	264.5	35.2	35.2
CANBERRA	300.8	300.8	26.8	27.1
RICHMOND	210.6	210.6	-18.8	31.0
TAMWORTH	249.3	249.3	57.1	57.1
TENTERFIELD	244.5	244.5	47.0	51.6
DWELLINGUP FOREST	382.1	382.1	-35.3	57.6
JACUP	338.1	338.1	82.4	82.4
MANJIMUP	343.7	343.7	-55.0	77.0
NAMBOUR DPI	-137.7	169.7	-27.8	51.1
EUCUMBENE COVE	209.7	209.7	28.1	33.7

Fig. 5 Annual cycle of the daily normal of DF based on SDI (blue) and KBDI (red) at Clare (South Australia), Launceston (Tasmania), and Bega (New South Wales).

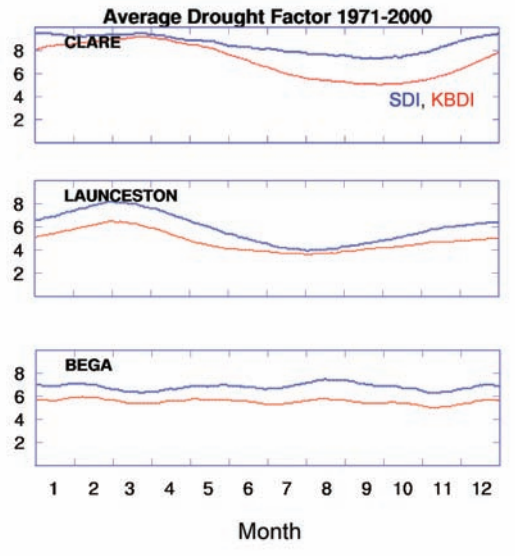

A similar but less dramatic behaviour can also be seen at Launceston where the KBDI and the SDI show similar numbers of days with lower drought factors (0-6), but during the summer using the SDI results in more days with high drought factors. Again the transition from low to high drought factors is more gradual for the KBDI. For this location the distributions of winter drought factors are similar for both the KBDI and the SDI, due to the similar normal winter soil moisture deficit conditions of KBDI and SDI (Finkele et al. 2006).

At Bega the distribution within the different drought factor classes shows little seasonality. However, the SDI shows a higher number of days within a month at the high drought factor end (9-10) of the distribution throughout the year (Fig. 6), similar to the behaviour shown for Clare. Again the transition from low to high drought factors is more gradual for the KBDI than for the SDI, especially in summer.

Applications

The initial motivation for developing the spatial DF products was to provide DF data in a form compatible

Fig. 6 **Frequency distributions within drought factor classes at Clare, Launceston and Bega for the mean annual cycle. Colours indicate number of days per month for which the DF is less than 6, 7, 8, 9 and 10. Left column shows drought factor classes based on KBDI (DFK) and right column drought factor classes based on SDI (DFS).**

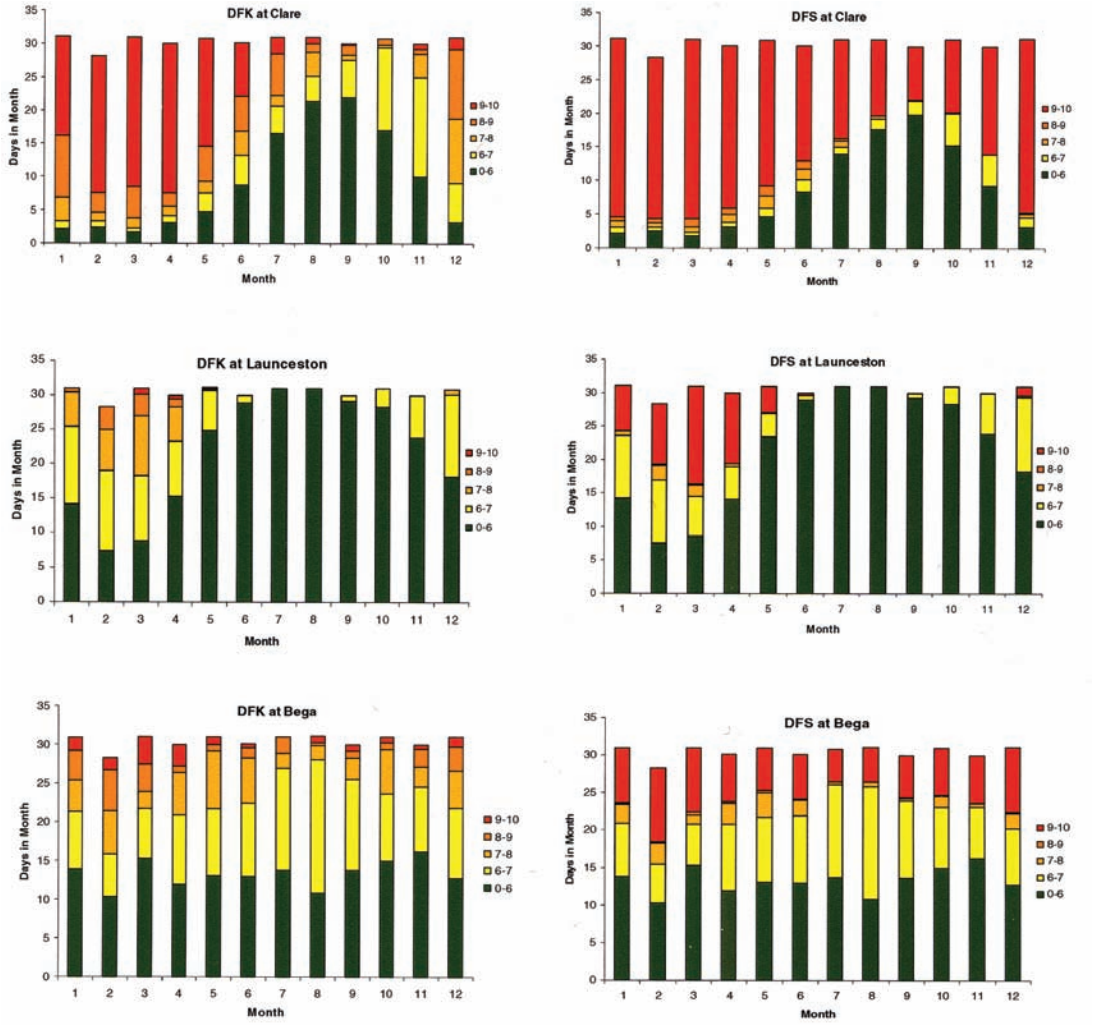

with the increasing quality and rich information content provided by current and emerging operational NWP systems. However, as the project developed, the opportunities provided by the 40-year archive of these fields based on the NCC daily rainfall and temperature analyses became more apparent. In addition, rather than the real-time DF data being simply incorporated into the FFDI calculations, the availability of fields of SDI in real time was seen to be of direct benefit to prescribed burn planning (e.g. Forestry Tasmania, 2000). Accordingly, several products have been provided to the Bureau's Regional Forecast Centres on an experimental basis, with the form of these products being developed in consultation with those offices.

As described earlier, in current operational practice the calculation of DF and the forecast of the FFDI is based on data from a network of observation sites. To emulate this currently available data to the forecasters, time series of drought factors and SMD at those observation sites are extracted from the time-series of gridded SMD/DF analyses. A typical product as presented to a forecaster is shown in Fig. 7 for Bendigo, Victoria. In these plots the last 12-month's evolution of SMD and DF based on the KBDI and the SDI formulations are plotted, as well as the annual cycle of the 30-year normals as a reference. As described earlier, we have chosen to use a SDI vegetation classification based on the leaf area index of the dominant vegetation type within the 0.1° or 0.25° grid

Fig. 7 **Extracted time series for Bendigo from the 0.25° grids for 26 May 2005 to 25 May 2006 of daily SMD and DF. Smooth curves represent the daily normal conditions (KBDI in red, SDI in blue). The soil moisture deficit plot shows the SDI for the grid-point assigned vegetation cover (SDI class C) as well as the additional SDI values for the alternative vegetation covers of light sparse forest (class B, pale blue) and dense forest (class E, green).**

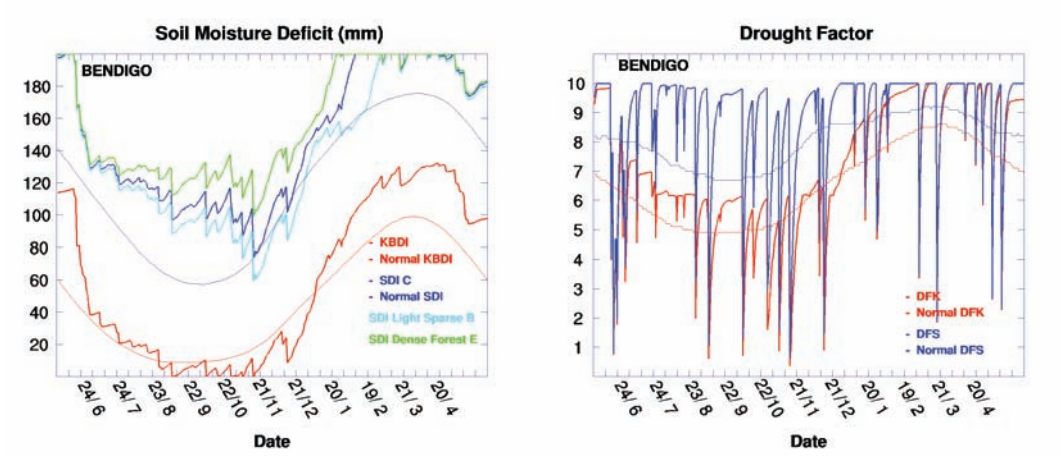

Fig. 8 **High resolution forecast of the FFDI for NSW valid for 0500 UTC 1 December 2004 using the gridded drought factor based on KBDI and forecast fields of hourly temperature, relative humidity and wind speed.**

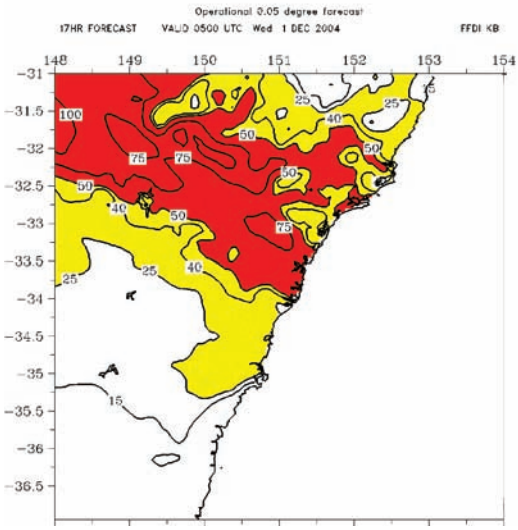

cell in these calculations. However, as was discussed briefly earlier, it may be of operational concern to assess the SDI for a significant, but non-dominant vegetation type. Thus to demonstrate the sensitivity of these estimates of SDI to the choice of vegetation type, two 'alternative SDI' time series are shown with one for sparse and one for dense vegetation cover and these additional curves are shown in the SMD panel of Fig. 7. However, no climatology or DF values are calculated from these alternative values.

The Bureau's highest resolution LAPS mesoscale NWP systems have grid spacings of approximately 5 km, and have domains covering southwestern Western Australia, central South Australia, Victoria/Tasmania, and central NSW, with model forecasts available at the full model resolution every hour. Combining these high-resolution NWP forecasts of near-surface temperature, relative humidity and wind speed with the current DF grids, and using the formula of Noble et al. (1980), a high spatial and temporal resolution forecast of the FFDI can be provided each day to forecasters. An example of such a forecast is shown in Fig. 8, the forecast being valid for the afternoon of 1 December 2004, a day on which extreme fire weather occurred north of Sydney ahead of, and with, the passage of a cool change. In Fig. 8 the yellow shading shows areas of the FFDI in the 'Very High' range, while red areas show 'Extreme' FFDI.

While the SMD/DF time-series presentation that meets forecaster requirements was shown in Fig. 7, the availability of a 40-year time series of daily gridded values allows a time series over that period to be presented. These long-term time series can be useful for climate analysis; for example, the number of days for which the SDI falls within prescribed burning guidelines might be useful in planning prescribed burning programs and resources. In addition, these time series clearly identify the droughts preceding the major fire seasons of 1983 (Ash Wednesday), and 2001/03, as can be seen in the example for Bendigo shown in Fig. 9. Further examples are presented in Finkele et al. (2006).

Fig. 9 **Time series of KBDI (red) and SDI (blue) soil moisture deficit in mm at Bendigo, Victoria, from 1966-2004, with values extracted from the daily gridded fields of these quantities.**

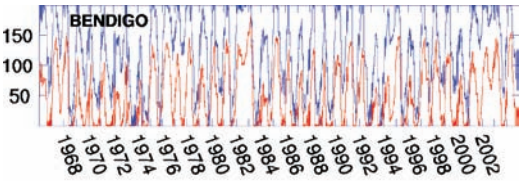

Conclusion

The development of a national gridded soil moisture deficit and Drought Factor product for fire weather applications has been described. These products are being produced daily and provide an alternative perspective to that provided by the current operational station-based values of these parameters, and make possible the provision of direct model output forecasts of the FFDI at high temporal and spatial resolution.

The comparison of the two available soil moisture deficit formulations (KBDI and SDI) showed that the main difference between the two schemes is due to the estimation of the evapotranspiration rather than to the infiltration/run-off process. The SDI generally leads to higher soil moisture deficits which in turn leads to a higher drought factor. Especially at warmer inland locations with sparse vegetation cover, the SDI is significantly higher than the KBDI due to the increased calculated evapotranspiration. The SDI may not be appropriate at such locations, as the evapotranspiration calculation does not take into account vegetation cover and is a linear function of maximum temperature with its coefficients derived at cooler mainly coastal locations.

The distribution within drought factor classes, which is important not only for extreme fire weather danger predictions but also for windows of opportunity for prescribed burning (low drought factors), is more gradual for the KBDI than for the SDI leading to more days with high drought factor for the SDI.

The availability of a 40-year daily time series of these analyses, based on the NCC's 40-year dataset of daily rainfall and maximum temperature analyses, provides a reference for the state of the drought factor at any time against the long-term climate. It offers many opportunities for long-term planning of resources needed for prescribed burn programs, for studying the variability of the FFDI, and has implications for seasonal fire weather forecasts and for investigating the effects of climate variability on fire weather regimes.

Acknowledgments

We would like to thank colleagues from BMRC for their assistance and contributions: Chermelle Engel for producing the initial Barnes analysis-based map of vegetation classification for SDI; Alan Wain for assistance with graphics for this paper and in particular for the production of the maps for the web; John Bally, Tony Bannister and Deryn Griffiths for numerous discussions on fire weather behaviour and the use of drought factors. Thanks also to Kevin Parkyn (Victorian Regional Office) and Grant Elliott (Western Australian Regional Office) who provided feedback on operational use of drought factors.

References

Cope, M.E., Hess, G.D., Lee, S., Tory, K.J., Azzi, M., Carras, J., Lilley, W., Manins, P.C., Nelson, P., Ng, L., Puri, K., Wong, N., Walsh, S. and Young, M. 2004. The Australian Air Quality Forecasting System. Part I: project description and early outcomes. *Jnl Appl. Met., 43*, 649–62.

Finkele, K., Mills, G.A., Beard, G. and Jones, D.A. 2006. National Daily Gridded Soil Moisture Deficit and Drought Factors for Use in Prediction of Forest Fire Danger Index in Australia. *Bureau of Meteorology Research Centre Research Report No. 119*, Bur. Met., Australia, 68 pp.

Forestry Tasmania 2000. *Using Low Intensity Fire in Land Management*. Forestry Tasmania, Hobart Australia, 63 pp.

Griffiths, D. 1998. Improved Formulae for the McArthur Forest Fire Danger Meter. *Meteorological Note 214*, Bur. Met., Australia, 11 pp.

Jones, D.A. 1999. Characteristics of Australian land surface temperature variability. *Theoretical and Applied Climatology, 63*, 11-31.

Keetch, J.J. and Byram, G.M. 1968. A Drought Factor Index for Forest Fire Control. *USDA Forest Service Research Paper SE-38*, 32 pp.

Luke, R.H. and McArthur, A.G. 1978. *Bushfires in Australia*. Australian Government Publishing Service, Canberra, 359 pp.

Mount, A.B. 1972. The Derivation and Testing of a Soil Dryness Index using Run-off Data. *Tasmanian Forestry Commission Bulletin No. 4*, 31 pp.

Noble, I.R., Barry, G.A.V. and Gill, A.M. 1980. McArthur's fire-danger meters expressed as equations. *Australian Journal of Ecology, 5*, 201-3.

Puri, K., Dietachmayer, G.D., Mills, G.A., Davidson, N.E., Bowen, R.A. and Logan, L.W. 1998. The new BMRC Limited Area Prediction System. LAPS. *Aust. Met. Mag., 47*, 203-23.

Sullivan, A. 2001. Review of the Operational Calculation of McArthur's Drought Factor. *CSIRO Forestry and Forest Products Client Report No. 921*, 46 pp.

Weymouth, G., Mills, G.A., Jones, D., Ebert, E.E. and Manton, M.J. 1999. A continental-scale daily rainfall analysis system. *Aust. Met. Mag., 48*, 169-79.